THE JOURNAL OF PHYSICAL CHEMISTRY Letters

Letter

pubs.acs.org/JPCL

Supramolecular Interactions in Secondary Plant Cell Walls: Effect of Lignin Chemical Composition Revealed with the Molecular Theory of Solvation

Rodrigo L. Silveira,[†,‡] Stanislav R. Stoyanov,*[,†,§,∥] Sergey Gusarov,[†] Munir S. Skaf,*[,‡] and Andriy Kovalenko*[,†,∥]

[†]National Institute for Nanotechnology, 11421 Saskatchewan Drive NW, Edmonton, Alberta T6G 2M9, Canada

[‡]Institute of Chemistry, University of Campinas, Caixa Postal 6154, Campinas CEP 13083-970, São Paulo, Brazil

[§]Department of Mechanical Engineering, University of Alberta, 4-9 Mechanical Engineering Building, Edmonton T6G 2G8, Alberta, Canada

[∥]Department of Chemical and Materials Engineering, University of Alberta, 9107 - 116 Street, Edmonton T6G 2V4, Alberta, Canada

Supporting Information

ABSTRACT: Plant biomass recalcitrance, a major obstacle to achieving sustainable production of second generation biofuels, arises mainly from the amorphous cell-wall matrix containing lignin and hemicellulose assembled into a complex supramolecular network that coats the cellulose fibrils. We employed the statistical-mechanical, 3D reference interaction site model with the Kovalenko−Hirata closure approximation (or 3D-RISM-KH molecular theory of solvation) to reveal the supramolecular interactions in this network and provide molecular-level insight into the effective lignin−lignin and lignin−hemicellulose thermodynamic interactions. We found that such interactions are hydrophobic and entropy-driven, and arise from the expelling of water from the mutual interaction surfaces. The molecular origin of these interactions is carbohydrate−π and $\pi-\pi$ stacking forces, whose strengths are dependent on the lignin chemical composition. Methoxy substituents in the phenyl groups of lignin promote substantial entropic stabilization of the ligno-hemicellulosic matrix. Our results provide a detailed molecular view of the fundamental interactions within the secondary plant cell walls that lead to recalcitrance.

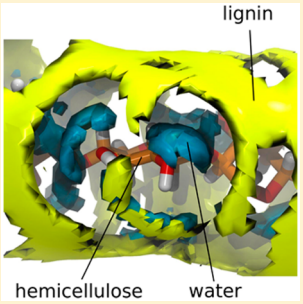

Lignocellulosic biomass constitutes a promising feedstock for producing biofuels and chemicals.[1] Because the three major components of plant biomass—cellulose, hemicellulose (Hc), and lignin—are organized in highly recalcitrant structures in plant cell walls (PCW), overcoming recalcitrance has been emphasized as being the most fundamental unsolved problem of plant-based green technologies.[1,2] The noncellulosic components of plant biomass, lignin and Hc, naturally assemble into a supramolecular 3D structure that protects cellulose microfibrils in secondary PCW and is considered a major reason for biomass recalcitrance.[1,3−5]

Lignin, the second most abundant biopolymer on earth, consists of phenylpropanoid units bonded together to form a complex 3D supramolecular network in the PCW and is the only large-scale renewable feedstock composed of aromatics.[6,7] Together with Hc, an amorphous heteropolysaccharide,[8] lignin fills the voids between cellulose microfibrils in the secondary PCW and creates a highly resistant barrier that impairs cellulose digestibility by reducing its accessibility to carbohydrate-modifying enzymes.

Because of the complexity of biomass, multidisciplinary efforts have been dedicated aiming for a picture of the lignocellulosic recalcitrance across multiple length scales.[7] Electron microscopy, electron tomography, and small-angle neutron scattering have shown that small lignin aggregates form within the bulk dilute-acid-pretreated biomass, coalesce into larger droplets, and redistribute to the PCW surfaces,[9,10] revealing a detailed view of the architecture of the pretreated biomass. Spatial distributions of lignin and cellulose in model samples have been assessed in 3D using time-of-flight secondary-ion mass spectroscopy to understand structural aspects underlying PCW recalcitrance.[11] A combination of small-angle neutron scattering and molecular dynamics (MD) simulations has shown that lignin aggregates possess a self-similar, multiscale structure with pores large enough to accommodate adsorbed cellulolytic enzymes.[12] In another study, molecular simulations have shown that lignin collapses at room temperature through an entropy-driven mechanism.[13] Also, MD simulations have shown interpenetration between lignin and Hc along the lignin−Hc interface,[14] suggesting an appreciable affinity between these PCW components. Although significant progress has been made toward our understanding of biomass recalcitrance, the underlying molecular mechanisms by which lignin chemical composition affects PCW recalcitrance remain elusive.

Received: October 29, 2014
Accepted: December 23, 2014
Published: December 23, 2014

DOI: 10.1021/jz502298q
J. Phys. Chem. Lett. 2015, 6, 206−211

Scheme 1. (a) Lignin Residues with Substituents R_1 and R_2 Determining the Lignin Type (shown in red); (b) Lignin Dimer, Highlighting the β-O-4′ Bond; (c) Lignin Monomer Used in the Calculations, with Both the 4-OH and β−OH Groups Replaced by CH_3O Groups; (d) Stick Representation of the Lignin and Hc Oligomers[a]

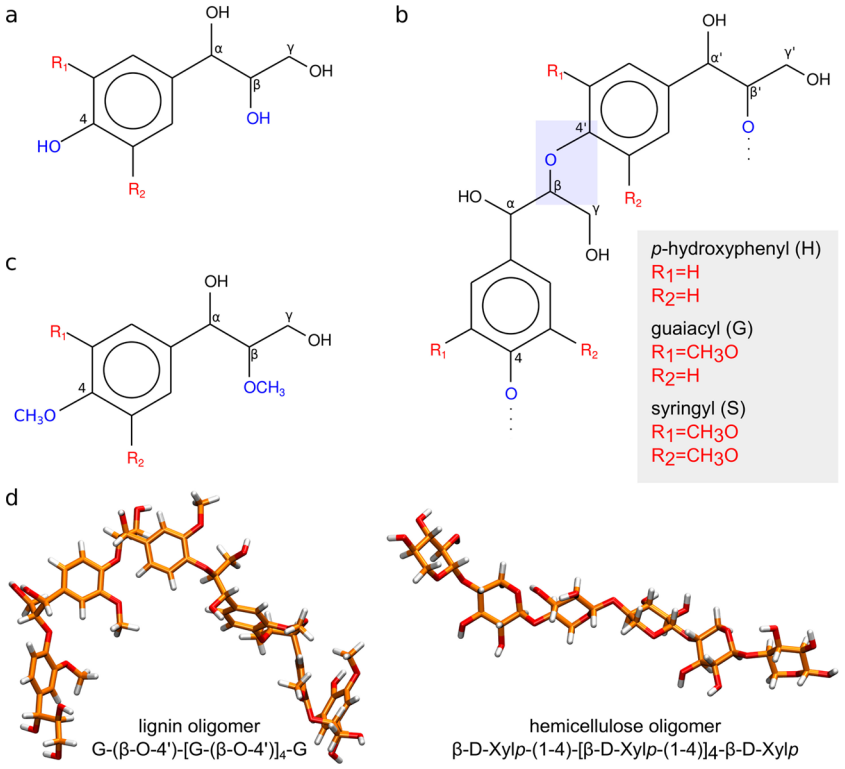

[a]Groups involved in the β-O-4′ bonding are represented in blue.

To understand the molecular basis of the recalcitrance forces within the PCW, we have recently employed the 3D-RISM-KH molecular theory of solvation to investigate the effect of Hc composition on the primary PCW strength and nanoarchitecture[15] as well as effective interactions between cellulose nanocrystals in aqueous electrolyte solutions, nonaqueous solvents, and ionic liquids.[16,17] Here we employ the 3D-RISM-KH theory to address the intermolecular forces present in the secondary PCW noncellulosic matrix, with a focus on the effect of lignin chemical composition on the thermodynamics of lignin−lignin and lignin−Hc effective interactions. From the first-principles of statistical mechanics, the 3D-RISM-KH method[18−20] bridges the gap between molecular structure and the effective forces and processes occurring in nanosystems on long time scales. The 3D-RISM-KH theory circumvents the major challenge of molecular simulations in obtaining adequate statistical sampling of solvation processes occurring on long time scales in complex solvents.

To assess lignin−Hc and lignin−lignin interactions, we consider Hc and lignin oligomers immersed in aqueous solutions of the lignin monomers *p*-hydroxyphenyl (H), guaiacyl (G), and syringyl (S) (Scheme 1a) at varying concentrations. Because the predominant lignin−lignin linkage in the lignin polymer is of the β-O-4′ type[21,22] with the β carbon atom bonded directly to the phenol oxygen atom (Scheme 1b), the linkage ether groups were replaced by methoxy groups (Scheme 1c) to construct monomers that better represent the polymer residues. These lignin monomer structures were optimized using molecular mechanics and used as an input in the dielectrically consistent RISM theory[23,24] coupled to the KH closure (DRISM-KH)[18−20] calculations for solvents comprising water and lignin monomers. The conformers (prepared using 10 ns long MD simulations) of the oligomers xylohexaose (a chain of six xylose monomers linked by $\beta(1 \rightarrow 4)$ glycosidic bonds) and hexaguaiacyl (6-residue guaiacyl chain linked by β-O-4′ bonds) were used as models for Hc and lignin, respectively (Scheme 1d). The CHARMM force field was used for Hc,[25] the TIP3P water model was modified for CHARMM,[26,27] and the CHARMM parameters of Petridis and Smith were used for lignin.[28] Subsequently, the 3D-RISM-KH theory was employed to compute the solvation thermodynamics of the oligomers as a function of lignin content and type in the aqueous environment.

The 3D-RISM-KH integral equations read

$$h_\gamma(\mathbf{r}) = \sum_\alpha \int d\mathbf{r}' c_\alpha(\mathbf{r} - \mathbf{r}') \chi_{\alpha\gamma}(|\mathbf{r}'|) \tag{1}$$

$$g_\gamma(\mathbf{r}) = \begin{cases} \exp(-u_\gamma(\mathbf{r})/(k_B T) + h_\gamma(\mathbf{r}) - c_\gamma(\mathbf{r})) & \text{for } g_\gamma(\mathbf{r}) \le 1 \\ 1 - u_\gamma(\mathbf{r})/(k_B T) + h_\gamma(\mathbf{r}) - c_\gamma(\mathbf{r}) & \text{for } g_\gamma(\mathbf{r}) > 1 \end{cases} \tag{2}$$

where $h_\gamma(\mathbf{r})$ and $c_\gamma(\mathbf{r})$ are, respectively, the 3D total and direct correlation functions, and $g_\gamma(\mathbf{r})$ is the 3D density distribution function of solvent site γ around the solute. The $\chi_{\alpha\gamma}(r)$ is the site−site radial susceptibility function of solvent that is an input calculated beforehand using the DRISM-KH theory,[18−20] and indices α and γ enumerate all interaction sites on all sorts of solvent species. The $u_\gamma(\mathbf{r})$ is the 3D interaction potential between the whole solute and solvent site γ, and $k_B T$ is the Boltzmann constant times the solution temperature.

The solvation free energy (SFE) $\Delta\mu$ is given by the closed analytical expression

DOI: 10.1021/jz502298q
J. Phys. Chem. Lett. 2015, 6, 206−211

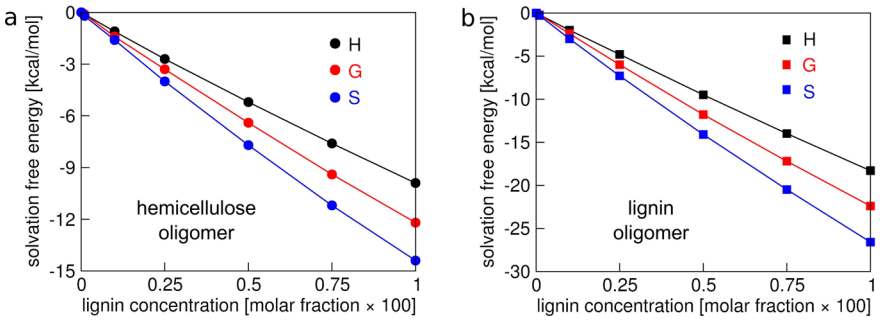

Figure 1. SFE of (a) Hc and (b) lignin oligomers in aqueous solutions of lignin monomers of different molar fractions relative to the SFE in pure water. The affinity of different lignin monomers for Hc and lignin oligomers is evident by the decrease in the SFE as lignin concentration is increased. Varying the lignin monomer type increases the strength of both (a) lignin−Hc and (b) lignin−lignin interactions in the order H < G < S.

$$\Delta\mu = \sum_{\gamma} \int_{V} \mathrm{d}\mathbf{r}\, \Phi_{\gamma}(\mathbf{r}) \tag{3}$$

$$\Phi_{\gamma}(\mathbf{r}) = \rho_{\gamma} k_{\mathrm{B}} T \left[\frac{1}{2} h_{\gamma}^{2}(\mathbf{r}) \Theta(-h_{\gamma}(\mathbf{r})) - c_{\gamma}(\mathbf{r}) - \frac{1}{2} h_{\gamma}(\mathbf{r}) c_{\gamma}(\mathbf{r}) \right] \tag{4}$$

where the sum goes over all of the sites of all solvent species, Θ is the Heaviside step function, and $\Phi_{\gamma}(\mathbf{r})$ is the 3D solvation free energy density (3D-SFED) coming from solvent interaction γ around the solute molecule. We notice that, by restricting the summation in eq 3 to solvent sites belonging to a given component (water or lignin), the SFE can be decomposed into components coming from each solvent species. These partial contributions carry the effective interactions of the solute (Hc and lignin oligomers) with the corresponding solvent species as well as all the solvent−solvent (water−water, lignin−lignin, and water−lignin) effective interactions through the susceptibility function in eq 1. The isochoric solvation entropy is computed as a central finite difference with temperature increment ΔT

$$\Delta s_{\mathrm{V}} = -\frac{1}{T}\left(\frac{\partial \Delta\mu}{\partial T}\right)_{\rho} \approx \frac{\Delta\mu(T + \Delta T, \rho) - \Delta\mu(T - \Delta T, \rho)}{2\Delta T} \tag{5}$$

A detailed description of the 3D-RISM-KH theory is available in refs 18−20.

The $\chi_{\alpha\gamma}(|\mathbf{r}|)$ was calculated for aqueous solutions of lignin monomers at concentration (molar fraction) ranging from 0 to 10^{-2} on a uniform grid of 8192 points with a spatial resolution of 0.1 Å at solution temperature 300 K, density 1.0 g·cm^{-3}, and dielectric constant 78.5. The 3D-RISM-KH eqs 1 and 2 were converged on a 3D grid of 128 × 128 × 128 points with a resolution of 0.5 Å in a 64 Å × 64 Å × 64 Å cubic box. For the entropy (eq 5), calculations were also carried out at temperatures 295 and 305 K. See the Supporting Information for computational details.

To assess the strength of the lignin-mediated interactions, we computed the SFE of the Hc and lignin oligomers in aqueous solutions of H, G, and S lignin monomers in varying concentrations. The presence of different lignin monomers in the solutions increases favorably the magnitude of the SFE of both the Hc and lignin oligomers by different amounts, indicating that the Hc−lignin and lignin−lignin interactions are thermodynamically favorable and dependent on the lignin composition.

Figure 1 shows the SFE of the Hc and lignin oligomers in the solutions of the three different lignin monomers as a function of monomer concentration, relative to the respective SFE of the Hc and lignin oligomers in pure water. The results indicate that as the lignin monomer concentration increases from 0 to 0.01 (expressed in molar fraction) the SFE magnitude for the Hc and lignin oligomers increases favorably by ∼10−15 and ∼17−27 kcal/mol, respectively, depending on lignin type. Such an increase in the SFE magnitude indicates that all lignin types provide effective stabilizing interactions to both Hc and lignin as well as that lignin has a high affinity for itself and hence a tendency to self-aggregate. The linear fitting slopes in Figure 1 show that the affinity (as expressed by the SFE) of Hc and lignin oligomers toward lignin increases in the order H < G < S. Moreover, we note that an increase in the number of methoxy groups in the phenyl rings of lignin (Scheme 1) leads to an increase in the SFE magnitude for the oligomers, indicating strengthening of both lignin−lignin and lignin−Hc effective interactions in aqueous medium.

An increase in the SFE magnitude for both Hc and lignin oligomers with an increase in the lignin concentration indicates that the stability of the secondary PCW, and hence its recalcitrance, is affected by the supramolecular interactions between lignin and Hc as well as by lignin self-aggregation. This is consistent with the experimental findings that a decreased lignin content can enhance biomass digestibility.[29] Lignin droplets that appear in PCW after dilute acid pretreatment provide compelling evidence of the lignin self-aggregation,[9] and our results indicate that the strength of such aggregates is a function of lignin composition. Also, lignin composition affects its interactions with Hc. This is important for biomass in which Hc removal is key for digestion, for instance, in switchgrass.[4] In such cases, the lignin composition could affect the pretreatment severity needed for Hc removal.

The effective interactions mediated by the S lignin are 25% stronger than those mediated by the G lignin, an effect that could be significant enough to modulate the PCW recalcitrance. Therefore, we suggest that the secondary PCW recalcitrance would be decreased as the S/G ratio is decreased. In fact, this trend has been observed experimentally by different groups for sugar cane and switchgrass.[30,31] Similarly, H-enriched lignin has been associated with decreased recalcitrance when compared with G- and S-enriched lignin,[32,33] which is consistent with our theoretical prediction that methoxy substituents in lignin enhance cell-wall stability. However, other reports show that improved biomass digestibility is associated with increased S/G ratio.[34,35] The controversy has been attributed to genetic, biochemical, and environmental factors involved in the experiments,[34] making the comparisons not straightforward. It is important to point out that biomass recalcitrance emerges

DOI: 10.1021/jz502298q
J. Phys. Chem. Lett. 2015, 6, 206−211

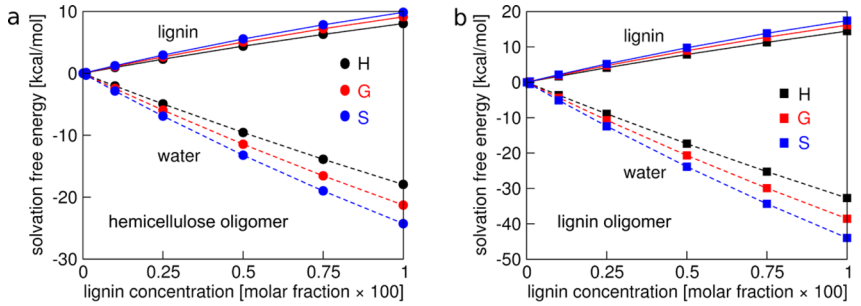

Figure 2. Partial contributions of lignin and water to the SFE of (a) Hc and (b) lignin oligomers as functions of the lignin concentration for the three types of lignin monomers. Dashed and solid lines correspond to water and lignin contributions, respectively. The partial contributions of water and lignin add up to the total solvation free energies presented in Figure 1

from several interdependent factors that are not all included in our model. Besides lignin content and composition, these factors include biomass porosity, the presence of lignin–carbohydrate complexes, lignin-induced enzyme inhibition, and cellulose crystallinity and accessibility.[1,2,22] The contribution of each of these factors has to be addressed individually to understand and control recalcitrance. Our results provide the relative strength of the supramolecular interactions of the PCW with no interference from other uncontrolled aspects that emerge at larger scales.

The fact that increasing the concentration and changing the chemical structure of the lignin result in similar effects on the SFE of both Hc and lignin oligomers strongly suggests that the lignin–lignin and lignin–Hc interactions have similar nature on the molecular level. To understand the driving force of the lignin-mediated supramolecular interactions, we computed the partial contributions of water and lignin monomers to the SFE of the Hc and lignin oligomers (Figure 2). These partial contributions were obtaining by splitting up the summation of eq 3 into two components running over the water and lignin interaction sites, respectively. The results show that the partial contribution of water to the SFE magnitude for Hc increases favorably as the lignin monomer concentration increases (Figure 2a), whereas the partial contribution of lignin increases unfavorably under these conditions. The lignin contribution accounts in part for the loss of translational and rotational entropy of the lignin monomers due to the interaction with Hc. Therefore, the thermodynamically favorable net effect is driven by the water contribution, which becomes larger as the lignin concentration is increased.

Moreover, the effect of the lignin composition is significantly more pronounced in the water contribution than in the lignin contribution itself (Figure 2a). The water contribution to the SFE magnitude increases in the same order as the total SFE, that is, H < G < S. The lignin–lignin interactions are also driven by the favorable increase in the partial contribution of water to the SFE magnitude, and the effect of the number of methoxy substitutions is manifested mainly through the water contribution (Figure 2b).

In Table 1, we list the SFE and solvation entropy of Hc and lignin oligomers in different lignin monomers at 300 K. The results indicate that the solvation entropy increases as the number of methoxy substitutions is increased (H < G < S) and accounts for most of the changes in the SFE, showing that the stabilization of the lignin–Hc and lignin–lignin interactions upon changing the lignin composition is due to an increase in the solvation entropy.

Table 1. SFE ($\Delta\mu$) and Solvation Entropy ($T\Delta s_V$, T = 300 K) of Hc and Lignin Oligomers in Aqueous Lignin Monomer Solutions at 0.01 (Molar Fraction), Relative to H Lignin

	Hc oligomer		lignin oligomer	
monomer	$\Delta\mu$ [kcal/mol]	$T\Delta s_V$ [kcal/mol]	$\Delta\mu$ [kcal/mol]	$T\Delta s_V$ [kcal/mol]
H	0	0	0	0
G	−2.2	2.2	−4.1	5.0
S	−4.5	3.8	−8.3	6.8

These results indicate that the Hc–lignin and lignin–lignin interactions are hydrophobic and suggest that the favorable contribution of water to the SFE is driven by dehydration of the monomer–oligomer interfaces. Furthermore, increasing the degree of methoxy substitutions in different lignin subtypes increases the hydrophobicity of the lignin monomers, which, in turn, increases the solvation entropies making methoxy-richer lignin monomers more effective in expelling water from hydrophobic surfaces. The relative hydrophobicity of the lignin monomers is also evidenced by the isothermal compressibility of the bulk lignin solutions (Supporting Information, Figure S1). Our results are consistent with the extensive MD simulations of Petridis et al., which predict lignin collapse by an entropy-driven mechanism at room temperature.[13] Solvent-driven association of lignin with cellulose was also observed in MD simulations.[36] In light of our results, lignin composition is likely to affect recalcitrance through lignin–cellulose interactions as well.

To obtain a molecular view of the supramolecular interactions that lead to the thermodynamic behavior described in the previous sections, we built the 3D-SFED (eq 4) isosurfaces (Figure 3). All isovalues are the same and defined by the full first solvation shell of water, which is to say that should a larger isovalue be applied the water 3D-SFED would show isosurfaces corresponding to the second hydration shell. The 3D-SFED contributions of water and different lignin types were computed separately so as to obtain a molecular level picture of the main effective interactions between the solute (Hc and lignin oligomers) and the solvent (water and lignin monomers).

Figure 3 presents the 3D-SFEDs for S lignin and water superimposed around the Hc and lignin oligomers, showing that water preferentially binds to Hc and lignin hydrogen-bonding sites, whereas lignin monomers spread over the hydrophobic surfaces of the oligomers, indicating that hydrophobic carbohydrate–π interactions predominate. Water is kept from reaching the hydrophobic surfaces by making more favorable interactions with the polar groups of the hemi-

DOI: 10.1021/jz502298q
J. Phys. Chem. Lett. 2015, 6, 206–211

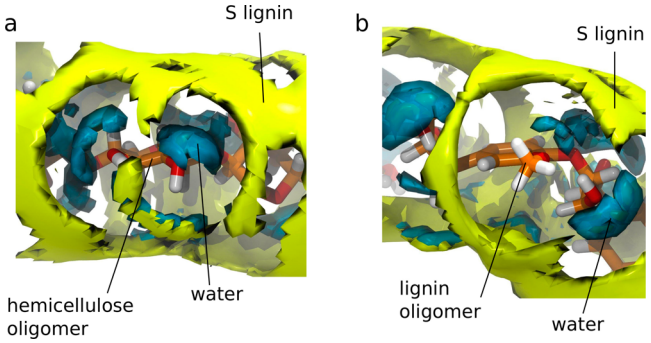

Figure 3. 3D-SFED isosurfaces of water (cyan) and syringyl lignin monomer (yellow) around the (a) Hc and (b) lignin oligomers (stick representation). The water 3D-SFED highlights the hydrogen bonds with polar groups. The syringyl 3D-SFED is markedly more spread than that of water, reflecting the nonspecific stacking hydrophobic interactions that predominate between lignin−Hc and lignin−lignin pairs.

cellulose and lignin oligomers. Such molecular pictures corroborate the idea that lignin minimizes its surface area in contact with water—causing it to coalesce and form spheres in pretreated biomass[21,22]—and further extend this mechanism to Hc−lignin interactions.

In this study, we revealed the supramolecular interactions between lignin and Hc, the two major heteropolymers in the noncellulosic matrix of the secondary PCW, and assessed the effects of lignin composition on the strength of such interactions. We found that the lignin−Hc and lignin−lignin interactions are very similar in character, both hydrophobic and nonspecific, which could be an essential requirement for assembly of the amorphous secondary PCW. As such, these interactions are driven by an entropic mechanism in which water is kept from contacting the hydrophobic surfaces. Also, we showed the effect of the chemical composition of lignin on the cohesive forces within the PCW and highlighted the importance of the methoxy substitutions in lignin for modulating the secondary PCW strength. The chemical composition of Hc is also likely an important factor when it comes to its integration into the secondary PCW; further studies are needed to address this aspect of biomass recalcitrance.

The computational results presented here can be validated experimentally with model compounds (e.g., Hc and lignin oligomers employed here) by using calorimetric techniques, such as isothermal titration calorimetry.[37] These experiments should provide the free energies associated with lignin−lignin and Hc−lignin interactions. Furthermore, more sophisticated model compounds could be employed to carefully assess PCW interactions. We emphasize that studying model compounds rather than the entire PCW could provide valuable insights further to the current understanding of the molecular aspects underlying lignocellulosic biomass recalcitrance.

Our findings are of crucial importance because of the urgent need for development of new technologies for biomass saccharification. This includes both rational design of new, inexpensive pretreatments and PCW engineering for improved digestibility, which ultimately depend on full comprehension of how the PCW recalcitrance emerges from the molecular and nanoscopic levels of description. In prospective, understanding this supramolecular system assembled by nature provides guidelines for biomimetic approaches to design of bio- and synthetic nanomaterials.

■ ASSOCIATED CONTENT

Supporting Information

Computational details and isothermal compressibility of lignin solutions. This material is available free of charge via the Internet at http://pubs.acs.org.

■ AUTHOR INFORMATION

Corresponding Authors

*E-mail: andriy.kovalenko@nrc-cnrc.gc.ca (A.K.).
*E-mail: skaf@iqm.unicamp.br (M.S.S.).
*E-mail: stoyanov@ualberta.ca (S.R.S.).

Notes

The authors declare no competing financial interest.

■ ACKNOWLEDGMENTS

This work was supported by the National Institute for Nanotechnology, the University of Alberta, the São Paulo Research Foundation FAPESP (Grant #2013/08293-7 to M.S.S. and #2014/10448-1 to R.L.S.) and CAPES (Grant #8663-11-4 to R.L.S.). S.R.S. thanks Dr. John M. Villegas for discussion. The computations were performed on the high-performance computing facilities of WestGrid − Compute/Calcul Canada.

■ REFERENCES

(1) Himmel, M. E.; Ding, S.-Y.; Johnson, D. E.; Adney, W. S.; Nimlos, M. R.; Brady, J. W.; Foust, T. D. Biomass Recalcitrance: Engineering Plants and Enzymes for Biofuels Production. *Science* **2007**, *315*, 804−807.

(2) Chundawat, S. P. S.; Beckman, G. T.; Himmel, M. E.; Dale, B. E. Deconstruction of Lignocellulosic Biomass to Fuels and Chemicals. *Annu. Rev. Chem. Biomol. Eng.* **2011**, *2*, 121−145.

(3) Ding, S.-Y.; Liu, Y.-S.; Zeng, Y.; Himmel, M. E.; Baker, J. O.; Bayer, E. A. How Does Plant Cell Wall Nanoscale Architecture Correlate with Enzymatic Digestibility? *Science* **2012**, *338*, 1055−1060.

(4) DeMartini, J. D.; Pattathil, S.; Miller, J. S.; Li, H.; Hahn, M. G.; Wyman, C. E. Investigating Plant Cell Wall Components that Affect Biomass Recalcitrance in Poplar and Switchgrass. *Energy Environ. Sci.* **2013**, *6*, 898−909.

(5) Achyuthan, K. E.; Achyuthan, A. M.; Adams, P. D.; Dirk, S. M.; Harper, J. C.; Simmons, B. A.; Singh, A. K. Supramolecular Self-Assembled Chaos: Polyphenolic Lignin's Barrier to Cost-Effective Lignocellulosic Biofuels. *Molecules* **2010**, *15*, 8641−8688.

(6) Ragauskas, A. J.; Beckham, G. T.; Biddy, M. J.; Chandra, R.; Chen, F.; Davis, M. F.; Davison, B. H.; Dixon, R. A.; Gilna, P.; Keller, M.; et al. Lignin Valorization: Improving Lignin Processing in the Biorefinery. *Science* **2014**, *344*, 1246843.

(7) Tuck, C. O.; Pérez, E.; Horváth, I. T.; Sheldon, R. A.; Poliakoff, M. Valorization of Biomass: Deriving More Value from Waste. *Science* **2012**, *337*, 695−699.

(8) Scheller, H. V.; Ulvskov, P. Hemicelluloses. *Annu. Rev. Plant. Biol.* **2010**, *61*, 263−289.

(9) Donohoe, B. S.; Decker, S. R.; Tucker, M. P.; Himmel, M. E.; Vinzant, T. B. Visualizing Lignin Coalescence and Migration Through Maize Cell Walls Following Thermochemical Pretreatment. *Biotechnol. Bioeng.* **2008**, *101*, 913−925.

(10) Pingali, S. V.; Urban, V. S.; Heller, W. T.; McGaughey, J.; O'Neill, H.; Foston, M.; Myles, D. A.; Ragauskas, A.; Evans, B. R. Breakdown of Cell Wall Nanostructure in Dilute Acid Pretreated Biomass. *Biomacromolecules* **2010**, *11*, 2329−2335.

(11) Jung, S.; Foston, M.; Kalluri, U. C.; Tuskan, G. A.; Ragauskas, A. J. 3D Chemical Image using TOF-SIMS Revealing the Biopolymer

DOI: 10.1021/jz502298q
J. Phys. Chem. Lett. 2015, 6, 206−211

Component Spatial and Lateral Distributions in Biomass. *Angew. Chem., Int. Ed.* **2012**, *51*, 12005−12008.
(12) Petridis, L.; Pingali, S. V.; Urban, V.; Heller, W. T.; O'Neill, H. M.; Foston, M.; Ragauskas, A.; Smith, J. C. Self-similar Multiscale Structure of Lignin Revealed by Neutron Scattering and Molecular Dynamics Simulation. *Phys. Rev. E* **2011**, *83*, 061911.
(13) Petridis, L.; Schulz, R.; Smith, J. C. Simulation Analysis of the Temperature Dependence of Lignin Structure and Dynamics. *J. Am. Chem. Soc.* **2011**, *133*, 20277−20287.
(14) Charlier, L.; Mazeau, K. Molecular Modeling of the Structural and Dynamical Properties of Secondary Plant Cell Walls: Influence of Lignin Chemistry. *J. Phys. Chem. B* **2012**, *116*, 4163−4174.
(15) Silveira, R. L.; Stoyanov, S. R.; Gusarov, S.; Skaf, M. S.; Kovalenko, A. Plant Biomass Recalcitrance: Effect of Hemicellulose Composition on Nanoscale Forces that Control Cell Wall Strength. *J. Am. Chem. Soc.* **2013**, *135*, 19048−19051.
(16) Stoyanov, S. R.; Gusarov, S.; Kovalenko, A. Multiscale Modeling of Solvation and Effective Interactions of Functionalized Cellulose Nanocrystals. In *Production and Applications of Cellulose Nanomaterials*; Postek, M. T., Moon, R. J., Rudie, A., Bilodeau, M., Eds.; TAPPI Press: Atlanta, GA, 2013; pp 147−150.
(17) Stoyanov, S. R.; Lyubimova, O.; Gusarov, S.; Kovalenko, A. Computational Modeling of the Structure Relaxation and Dispersion Thermodynamics of Pristine and Modified Cellulose Nanocrystals in Solution. *Nord. Pulp Paper Res. J.* **2014**, *29*, 144−155.
(18) Kovalenko, A.; Hirata, F. Self-consistent Description of a Metal-Water Interface by the Kohn-Sham Density Functional Theory and the Three-dimensional Reference Interaction Site Model. *J. Chem. Phys.* **1999**, *110*, 10095−10112.
(19) Kovalenko, A. Three-Dimensional RISM Theory for Molecular Liquids and Solid-Liquid Interfaces. In *Molecular Theory of Solvation*; Hirata, F., Ed.; Understanding Chemical Reactivity *24*; Kluwer Academic Publishers: Dordrecht, Netherlands, 2003; pp 169−275.
(20) Kovalenko, A. Multiscale Modeling of Solvation in Chemical and Biological Nanosystems and in Nanoporous Materials. *Pure Appl. Chem.* **2013**, *85*, 159−199.
(21) Boerjan, W.; Ralph, J.; Baucher, M. Lignin Biosynthesis. *Annu. Rev. Plant Biol.* **2003**, *54*, 519−546.
(22) Pu, Y.; Hu, F.; Huang, F.; Davison, B. H.; Ragauskas, A. J. Assessing the Molecular Structure Basis for Biomass Recalcitrance During Dilute Acid and Hydrothermal Pretreatments. *Biotechnol. Biofuels* **2013**, *6*, 15.
(23) Perkyns, J. S.; Pettitt, B. M. A Dielectrically Consistent Interaction Site Theory for Solvent-Electrolyte Mixtures. *Chem. Phys. Lett.* **1992**, *190*, 626−630.
(24) Perkyns, J. S.; Pettitt, B. M. Site-site Theory for Finite Concentration Saline Solutions. *J. Chem. Phys.* **1992**, *97*, 7656−7666.
(25) Guvench, O.; Greene, S. N.; Kamath, G.; Brady, J. W.; Venable, R. M.; Pastor, R. W.; MacKerell, A. D., Jr. Additive Empirical Force Field for Hexopyranose Monosaccharides. *J. Comput. Chem.* **2008**, *29*, 2543−2564.
(26) Jorgensen, W. L.; Chandrasekhar, J.; Madura, J. D.; Impey, R. W.; Klein, M. L. Comparison of Simple Potential Functions for Simulating Liquid Water. *J. Chem. Phys.* **1983**, *79*, 926−935.
(27) MacKerell, A. D., Jr.; Bashford, D.; Bellott, R. L.; Dunbrack, R. L., Jr.; Evanseck, J. D.; Field, M. J.; Fischer, S.; Gao, J.; Guo, H.; Ha, S.; et al. All-Atom Empirical Potential for Molecular Modeling and Dynamics Studies of Proteins. *J. Phys. Chem. B* **1998**, *102*, 3586−3616.
(28) Petridis, L.; Smith, J. C. A Molecular Mechanics Force Field for Lignin. *J. Comput. Chem.* **2009**, *30*, 457−467.
(29) Chen, F.; Dixon, R. A. Lignin Modification Improves Fermentable Sugar Yields for Biofuel Production. *Nat. Biotechnol.* **2007**, *25*, 759−761.
(30) Hung, J. H.; Fouad, W. M.; Vermerris, W.; Gallo, M.; Altpeter, F. RNAi Suppression of Lignin Biosynthesis in Sugarcane Reduces Recalcitrance for Biofuel Production from Lignocellulosic Biomass. *Plant Biotechnol. J.* **2012**, *10*, 1067−1076.
(31) Fu, C.; Mielenz, J. R.; Xiao, X.; Ge, Y.; Hamilton, C. Y.; Rodriguez, M., Jr.; Chen, F.; Foston, M.; Ragauskas, A.; Bouton, J.; et al. Genetic Manipulation of Lignin Reduces Recalcitrance and Improves Ethanol Production from Switchgrass. *Proc. Natl. Acad. Sci. U.S.A.* **2011**, *108*, 3803−3808.
(32) Bonawitz, N. D.; Kim, J. I.; Tobimatsu, Y.; Ciesielski, P. N.; Anderson, N. A.; Ximenes, E.; Maeda, J.; Ralph, J.; Donohoe, B. S.; Ladisch, M.; Chapple, C. Disruption of Mediator Rescues the Stunted Growth of a Lignin-Deficient *Arabidopsis* Mutant. *Nature* **2014**, *509*, 376−380.
(33) Ziebell, A.; Gracom, K.; Katahira, R.; Chen, F.; Pu, Y.; Ragauskas, A.; Dixon, R. A.; Davis, M. Increase in 4-Coumaryl Alcohol Units During Lignification in Alfafa (*Medicago sativa*) Alters the Extractability and Molecular Weight of Lignin. *J. Biol. Chem.* **2010**, *285*, 38961−38968.
(34) Li, X.; Weng, J.-K.; Chapple, C. Improvement of Biomass Through Lignin Modification. *Plant J.* **2008**, *54*, 569−581.
(35) Mansfield, S. D. Solutions for Dissolution — Engineering Cell Walls for Deconstruction. *Curr. Opin. Biotechnol.* **2009**, *20*, 286−294.
(36) Lindner, B.; Petridis, L.; Schulz, R.; Smith, J. C. Solvent-driven Preferential Association of Lignin with Regions of Crystalline Cellulose in Molecular Dynamics Simulation. *Biomacromolecules* **2013**, *14*, 3390−3398.
(37) Kabiri, M.; Unsworth, L. D. Application of Isothermal Titration Calorimetry for Characterizing Thermodynamic Parameters of Biomolecular Interactions: Peptide Self-Assembly and Protein Adsorption Case Studies. *Biomacromolecules* **2014**, *15*, 3463−3473.

DOI: 10.1021/jz502298q
J. Phys. Chem. Lett. 2015, 6, 206−211